Available online at www.sciencedirect.com

ScienceDirect

Ceramics International 39 (2013) 9823–9828

CERAMICS INTERNATIONAL

www.elsevier.com/locate/ceramint

Photoluminescence properties in Sm doped $Bi_{1/2}Na_{1/2}TiO_3$ ferroelectric ceramics

T. Wei[a,*], F.C. Sun[a], C.Z. Zhao[b], C.P. Li[c], M. Yang[a], Y.Q. Wang[a]

[a]College of Science, Civil Aviation University of China, Tianjin 300300, China
[b]School of Electronics and Information Engineering, Tianjin Polytechnic University, Tianjin 300160, China
[c]School of Electronics Information Engineering, Tianjin Key Laboratory of Film Electronic and Communication Devices, Tianjin University of Technology, Tianjin 300384, China

Received 14 April 2013; received in revised form 24 May 2013; accepted 24 May 2013
Available online 31 May 2013

Abstract

Sm^{3+} ions doped $Bi_{1/2}Na_{1/2}TiO_3$ (BNTO: xSm^{3+}) polycrystalline samples with different Sm^{3+} concentrations were synthesized through the solid-state reaction method. Their microstructural, photoluminescence, and ferroelectric (FE) properties were investigated. Strong reddish-orange emission centered at 597 nm has been successfully observed at room temperature. More importantly, the strong emission of BNTO: xSm^{3+} can be excited by both blue light and near ultraviolet radiation which indicates that BNTO: xSm^{3+} can act as a potential phosphor. Furthermore, the optimized photoluminescence is realized in BNTO: xSm^{3+} with $x=0.02$ sample which also shows relatively good ferroelectric properties.

Keywords: X-ray diffraction; Photoluminescence; Ferroelectricity

1. Introduction

White light-emitting diodes (LEDs), as a potential candidate for replacement of conventional incandescent and fluorescent lamps, have become a focus of many researches owing to their significant power saving, higher luminous efficiency, longer lifetime, and reliability [1,2]. Three different approaches can be employed to realize white light based on LEDs [3]. It is believed that white LEDs fabricated by blue LED chips combined with yellow-emitting phosphors or ultraviolet (NUV) LED chips coated with red—green—blue (RGB) tri-color phosphors might be the direction of solid-state lighting (SSL) development for their high efficiency and easy fabrication [4,5]. Currently, it is important to explore good phosphors in which the strong absorption locates in the blue or NUV spectral region and strong light emission locates in the visible range.

Recently, rare-earth doped ABO_3 perovskite ferroelectric materials have been investigated owing to their potential application as emitting phosphors or optical-electro-material [6—9]. Among them, ferroelectric $Bi_{1/2}Na_{1/2}TiO_3$ (BNTO), with a complicated ABO_3 structure (A=Bi, Na and B=Ti), is considered as one of the good candidates because BNTO shows a low deposition temperature and a large remanent polarization [10—12]. Furthermore, mixed $Bi_{1/2-x}RE_xNa_{1/2}TiO_3$, where RE is the rare earth element, is attractive to researchers because of its excellent and rich physics relative to pure BNTO. Wang et al. reported that greatly improved luminescence behavior can be realized in Pr^{3+} doped BNTO ferroelectric ceramics synthesized by solid-state reaction [13]. Moreover, Bao et al. reported the strong red emission of Pr^{3+}-doped BNTO thin films prepared by using the chemical solution deposition method [14]. Very recently, remarkable enhancement of the red emission intensity of Pr^{3+}-doped BNTO ceramics by modifying their ferroelectric remanent polarization has been reported by Jia et al. [15].

It is clear that BNTO with low symmetry perovskite structure can act as a very promising host material for the production of red phosphor for white LEDs. However, to the best of our knowledge, besides the Pr doped BNTO, there are few luminescence studies on rare earth doped BNTO

*Corresponding author. Tel.: +86 15122848807; fax: +86 2224092514.
E-mail address: weitong.nju@gmail.com (T. Wei).

0272-8842/$ - see front matter © 2013 Elsevier Ltd and Techna Group S.r.l. All rights reserved.
http://dx.doi.org/10.1016/j.ceramint.2013.05.094

compound [13—15]. Therefore, to obtain a deep comprehension of BNTO system, now, it is a proper time to address the luminescence feature of BNTO doped by other rare earth ions. As we know, Sm^{3+} is an important activator ion of inorganic materials which can also play the role of red emission centers [16,17]. Thus, it is of interest and significance to investigate luminescence properties of Sm^{3+} doped BNTO system.

In the present study, Sm^{3+} doped BNTO ceramics (BNTO: $x$$Sm^{3+}$) with different concentrations were synthesized through the solid state reaction method. The luminescence properties of BNTO: $x$$Sm^{3+}$ were first reported. Strong reddish-orange emission has been successfully observed at room temperature. More importantly, the reddish-orange emission of Sm^{3+} doped BNTO ceramics can be excited by both blue light and NUV radiation. Furthermore, the optimal emission intensity was obtained when x=0.02 for BNTO: $x$$Sm^{3+}$ system. In addition, BNTO: $x$$Sm^{3+}$ with x=0.02 also shows well defined polarization—electric field hysteresis loops. It is believed that BNTO: $x$$Sm^{3+}$ with x=0.02 may act as a potentially multifunctional optical-electro-material.

2. Experimental details

The polycrystalline $Bi_{1/2-x}Na_{1/2}TiO_3$: $x$$Sm^{3+}$ (BNTO: $x$$Sm^{3+}$) ($x$=0.0, 0.005, 0.01, 0.02, 0.04, 0.06, 0.08, 0.12, and 0.16) ceramics were synthesized by conventional solid-state reaction [18]. Highly purified powders Bi_2O_3 (99%), Sm_2O_3 (99.99%), Na_2CO_3 (99.8%) and TiO_2 (99%) were weighed to prepare BNTO: $x$$Sm^{3+}$ samples. In order to compensate for the Bi and Na vaporization during the thermal annealing, Bi_2O_3 and Na_2CO_3 were 4% and 5% excesses in the starting powder, respectively. After mixing by milling in alcohol for 24 h using agate pots and agate balls in a planetary mill, the as-prepared powders were dried and then calcined at 850 °C for 4 h. The resultant powders were reground and pelletized under 15 MPa pressure into disks of 13 mm in diameter and sintered at 1150 °C for 4 h.

Phase analysis and crystal structures of the prepared BNTO: $x$$Sm^{3+}$ samples were evaluated using X-ray diffraction (XRD) at room temperature. A scanning electron microscope (SEM) (Nova NanoSEM 430) was used to characterize the microstructures. The photoluminescence (PL) spectra at room temperature were recorded by using a Jobin Yvon HR320 fluorescence spectrophotometer. Electrodes were fabricated with fired-on silver paste for electrical measurements. The ferroelectric (FE) behaviors were measured with a Radiant Precision Multiferroic Tester (Radiant Technologies Ltd., Albuquerque, NM) in a standard mode.

3. Results and discussions

XRD patterns of BNTO: $x$$Sm^{3+}$ ceramics with x ranging from 0.0 to 0.16 are given in Fig. 1(a). The diffraction peaks of BNTO: $x$$Sm^{3+}$ with different Sm^{3+} concentrations can be indexed according to the standard diffraction pattern data of single BNTO phase and agree well with the Joint Committee for Powder Diffraction Standards card (No. 36-340) [15]. No other secondary phases, such as Bi_2O_3, $NaCO_3$, Sm_2O_3, and TiO_2, are detected in the current XRD pattern. The XRD result indicates that the Sm^{3+} ions were completely dissolved in the BNTO host lattice.

Compared with pure $Bi_{0.5}Na_{0.5}TiO_3$ phase, obvious shifts are observed in the peak positions for the BNTO: $x$$Sm^{3+}$ samples. One can see in Fig. 1(a) that the (202) diffraction peak shifts to high angle side with increase of Sm^{3+} ions concentration. Referring to the ion radius of Sm^{3+} (1.24 Å, CN12) and Bi^{3+} (1.30 Å, CN12) [19], lattice distortion associated with the doping of Sm^{3+} at Bi^{3+} site can be introduced in the BNTO: $x$$Sm^{3+}$ system.

To further characterize the microstructure, scanning electron microscopy (SEM) was carried out for the current BNTO: $x$$Sm^{3+}$ system. Fig. 1 also presents typical SEM images of BNTO: $x$$Sm^{3+}$ with x=0.0 (b), 0.01 (c), 0.04 (d), and 0.08 (e). It can be seen that all the ceramic samples show similar SEM micrographs. Rectangular-like grains can be observed. With the increase of Sm^{3+} concentration, the size of grains starts to decrease. It can be attributed to the fact that partial substitution of Sm^{3+} at Bi^{3+} sites can inhibit the growth of rectangular-like grains of BNTO: $x$$Sm^{3+}$ system.

Now we focus on the luminescence properties of BNTO: $x$$Sm^{3+}$ system. To understand the excitation paths of Sm^{3+} ions, Fig. 2 gives the photoluminescence excitation (PLE) spectra associated with different Sm^{3+} concentrations of BNTO: $x$$Sm^{3+}$ samples by monitoring the 597 nm emission. One can see that obvious excitation peaks for BNTO: $x$$Sm^{3+}$ (x≠0.0) are detected, and the PLE spectra show similar characteristic excitation peaks. The remarkably strong and sharp excitation peaks in the wavelength range of 390—510 nm are owing to the typical f—f absorption of Sm^{3+} [20—22]. The intense broad excitation band between 450 and 510 nm should be attributed to the transitions from the $^6H_{5/2}$ ground state to the $^4I_{13/2}$, $^4I_{11/2}$, $^4M_{15/2}$, $^4I_{9/2}$, and $^4G_{7/2}$ excited states of Sm^{3+} as shown in Fig. 2. On the other hand, the sharp excitation peaks around 406, 420, and 440 nm correspond with the transitions from the $^6H_{5/2}$ ground state to the $^4F_{7/2}$, $(^6P, ^4P)_{5/2}$, and $^4G_{9/2}$ excited states of Sm^{3+}. No shifts of the excited peaks for all of the BNTO: $x$$Sm^{3+}$ samples are observed in Fig. 2. It should be noted that the remarkable excitation band (450—510 nm) locates around the emission wavelength of commercial blue LEDs (450—470 nm) which indicates that BNTO: $x$$Sm^{3+}$ can act as a potential blue exciting phosphor [3]. Furthermore, what is interesting is that BNTO: $x$$Sm^{3+}$ can also be excited by near ultraviolet (NUV) LEDs (350—420 nm) referring to the strong and sharp excitation peaks at 407 nm and 420 nm which indicates that BNTO: $x$$Sm^{3+}$ can also act as a potential NUV exciting phosphor.

Fig. 3 presents the photoluminescence (PL) spectra with different Sm^{3+} ions concentrations excited by blue light with wavelength 466 nm at room temperature. Under the resonant excitation at 466 nm, the broad bands peaking around 563 nm, 597 nm, 644 nm, and 708 nm owing to intra f—f transitions of Sm^{3+} ions are obtained. These bands in PL spectra present characteristic $^4G_{5/2} \rightarrow {}^6H_J$ (J=5/2, 7/2, 9/2, and 11/2) transitions. Among them, the transition at 597 nm ($^4G_{5/2} \rightarrow {}^6H_{7/2}$) has the

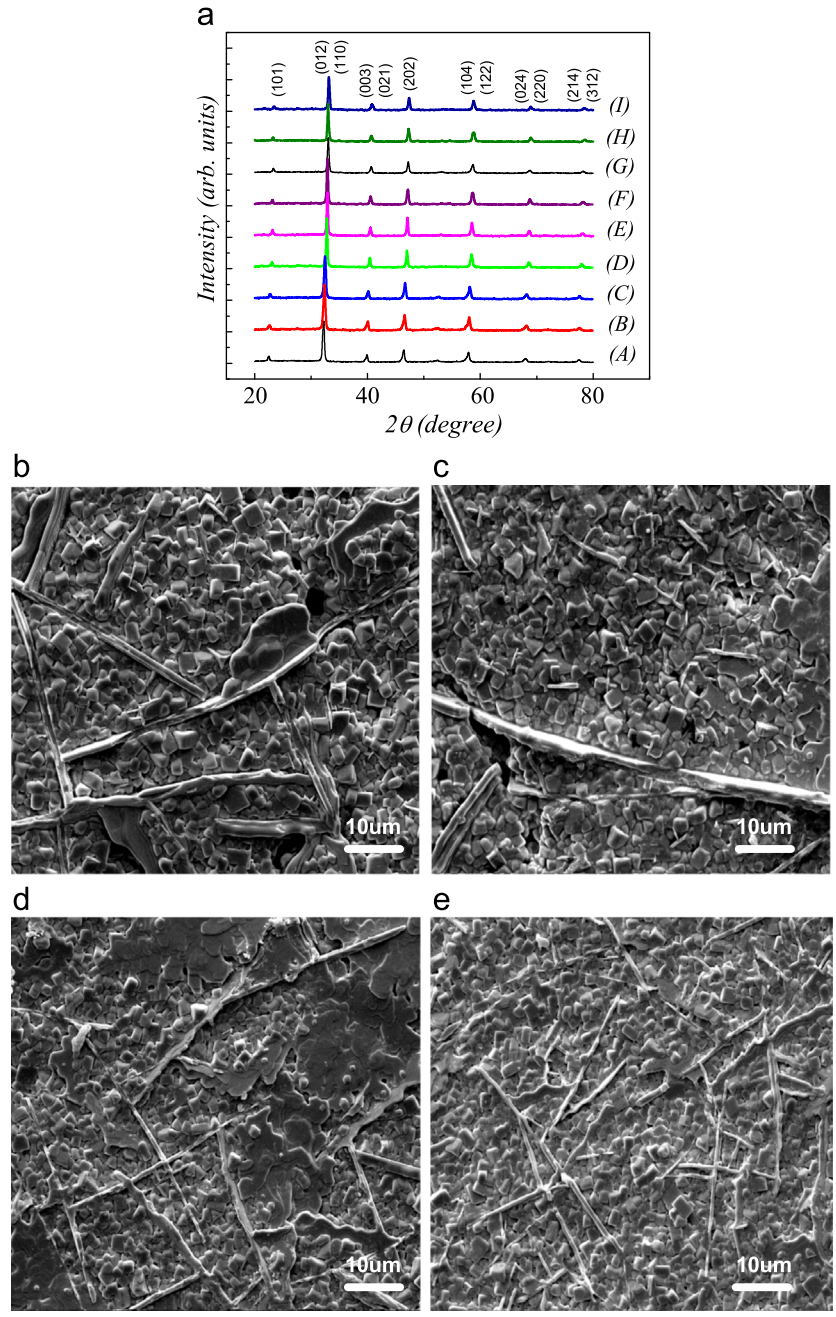

Fig. 1. XRD patterns (a) of BNTO: $x\mathrm{Sm}^{3+}$ ceramics with different Sm^{3+}-doped concentrations: (A) $x=0.0$, (B) $x=0.005$, (C) $x=0.01$, (D) $x=0.02$, (E) $x=0.04$, (F) $x=0.06$, (G) $x=0.08$, (H) $x=0.12$, and (I) $x=0.16$. SEM images of BNTO: x Sm^{3+} with $x=0.0$ (b), 0.01 (c), 0.04 (d), and 0.08 (e).

maximum intensity which corresponds to the reddish-orange emission. To clearly illustrate the PL process, the inset of Fig. 5 represents a simplified energy level diagram involved in the emission process of Sm^{3+} ions in BNTO: $x\mathrm{Sm}^{3+}$ phosphor.

It is believed that the $^4G_{5/2}\rightarrow{}^6H_{5/2}$ (563 nm) transition is a magnetic dipole allowed transition and its intensity hardly varies with the environment of the Sm^{3+} ions. The $^4G_{5/2}\rightarrow{}^6H_{7/2}$ (597 nm) transition is a partly magnetic and partly forced electric-dipole transition; however, the $^4G_{5/2}\rightarrow{}^6H_{9/2}$ (644 nm) transition is a purely electric dipole transition which is sensitive to the crystal field [23—25]. Therefore, the ratio (R) of the intensity of $^4G_{5/2}\rightarrow{}^6H_{9/2}$ to that of $^4G_{5/2}\rightarrow{}^6H_{5/2}$ can be used to evaluate the surrounding of the Sm^{3+} coordination. Fig. 4 gives the variation of R value with x. One can see that there is a growing tendency of R value on the whole. For example, the R value for $x=0.005$ of BNTO: $x\mathrm{Sm}^{3+}$ is only about 0.74; however, the R value reaches up to about 0.85 when $x=0.16$. The higher R value in BNTO: $x\mathrm{Sm}^{3+}$ phosphor indicates the enhanced lattice distortion which is consistent with the results of XRD in Fig. 1.

Furthermore, to evaluate the performance of BNTO: $x\mathrm{Sm}^{3+}$ as a potential NUV exciting phosphor, the PL spectra of

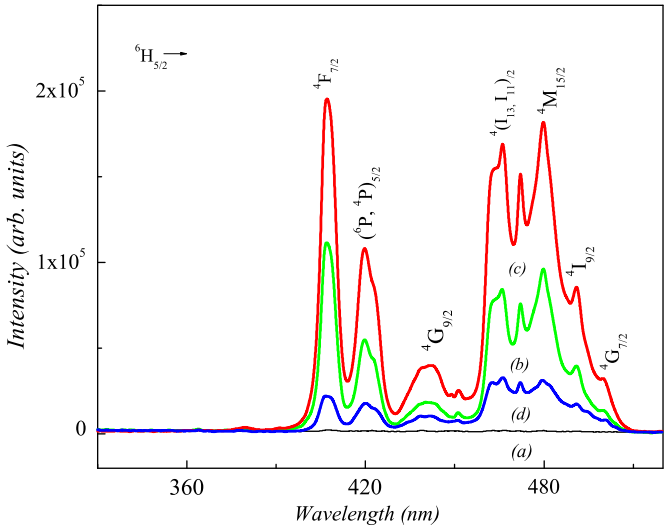

Fig. 2. Photoluminescence excitation (PLE) spectra monitored at 597 nm of BNTO: xSm^{3+} with x=0.0 (a), 0.005 (b), 0.02 (c), and 0.08 (d).

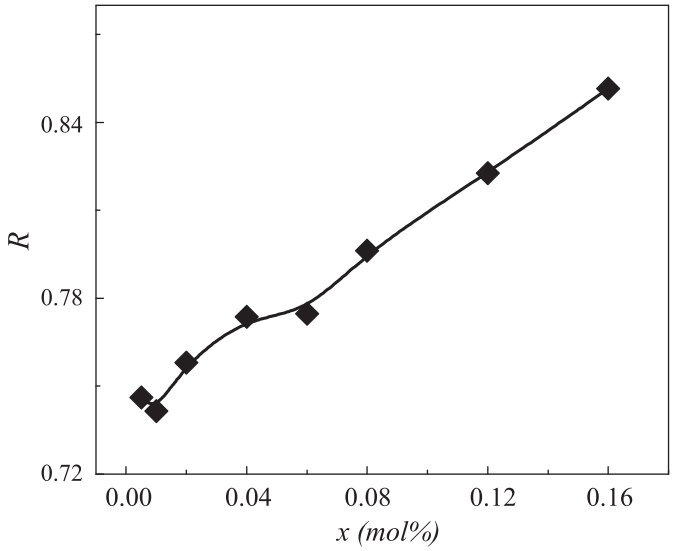

Fig. 4. Variation of R with x for BNTO: xSm^{3+} system. The smooth solid curve is guide for eyes.

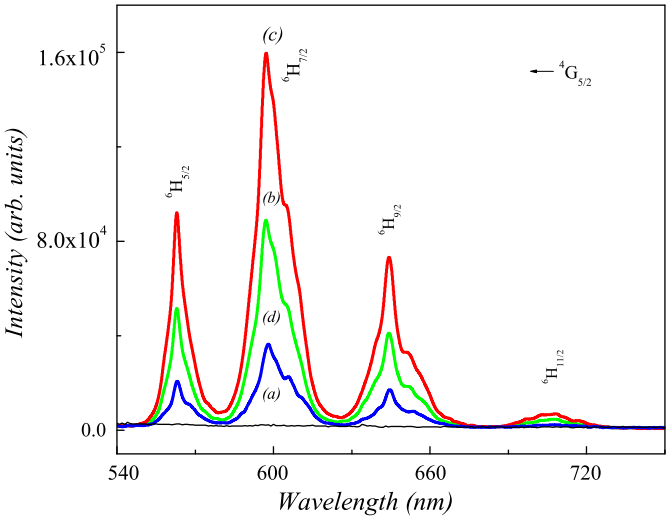

Fig. 3. Photoluminescence (PL) spectra of BNTO: xSm^{3+} samples with x=0.0 (a), 0.005 (b), 0.02 (c), and 0.08 (d), excited at 466 nm.

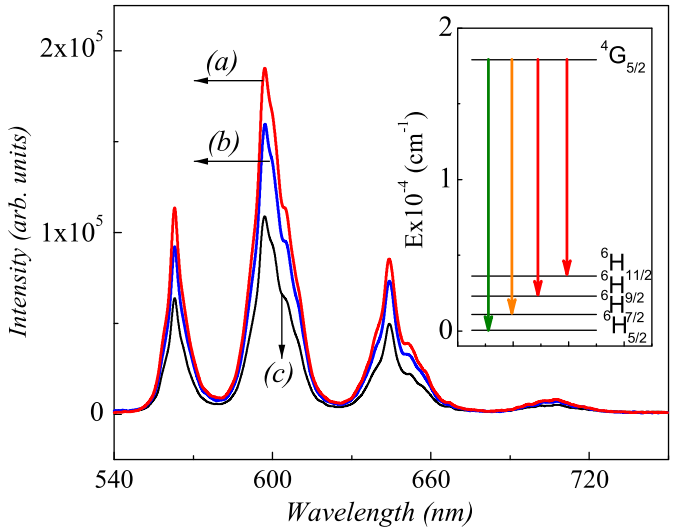

Fig. 5. Photoluminescence (PL) spectra of BNTO: xSm^{3+} samples with x=0.02 excited at 407 nm (a), 0.02 excited at 466 nm (b), and 0.005 excited at 407 nm (c). The inset of Fig. 5 shows a simplified energy level diagram of Sm^{3+}.

BNTO: xSm^{3+} with x=0.005 and 0.02 excited by NUV light with wavelength 407 nm at room temperature were also measured and are presented in Fig. 5. In addition, the PL spectrum of BNTO: xSm^{3+} with x=0.02 excited by blue light with 466 nm is also plotted in Fig. 5 for clear comparison. It is clear that the spectra of BNTO: xSm^{3+} (x=0.005 and 0.02) irradiated with NUV (407 nm) radiation show strong and sharp emission peaks which have similar feature with that of PL spectrum of BNTO: xSm^{3+} (x=0.02) excited by blue light 466 nm. The above results confirm that BNTO: xSm^{3+} can act as a potential phosphor excited by commercial blue and NUV light.

At this stage, considering that the luminescence performance of the phosphors depends mainly on the concentration of activator ions, the identification of optimum doping concentration is necessary. Fig. 6 gives the variation of the emission ($^4G_{5/2}\rightarrow{}^6H_{7/2}$, 597 nm) and excitation ($^6H_{5/2}\rightarrow{}^4(I_{13}, I_{11})_{/2}$, 466 nm) intensity with x. It is clear that emission and excitation light intensity reaches a maximum value at x=0.02, and then decreases with an increase in x due to the concentration quenching effect. This is because as the concentration of the luminescent ions increases, the distance between them decreases and causes the non-radiative energy transfer from one activator to another activator ion leading to the lowering of fluorescence intensity [26]. From the above results, BNTO: xSm^{3+} with x=0.02 sample exhibits optimized photoluminescence.

Besides the PL properties, BNTO: xSm^{3+} is also an important ferroelectric (FE) material. Thus, to confirm the multifunctional properties of BNTO: xSm^{3+}, FE measurement

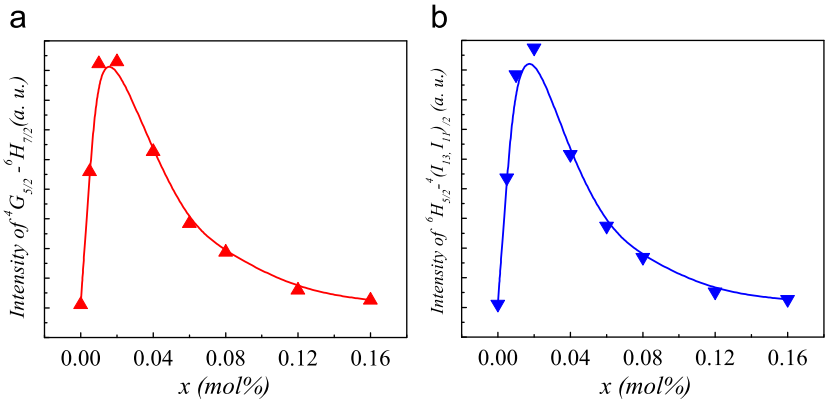

Fig. 6. Variation of emission ($^4G_{5/2}\rightarrow{}^6H_{7/2}$) (a) and excitation ($^6H_{5/2}\rightarrow{}^4(I_{13}, I_{11})_{/2}$) (b) intensity of BNTO: xSm^{3+} versus x.

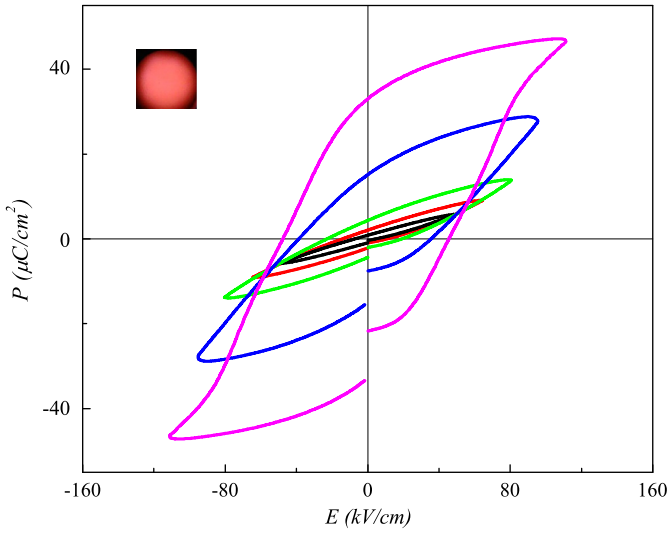

Fig. 7. Polarization—electric field (P—E) hysteresis loops of BNTO: xSm^{3+} with $x=0.02$ at room temperature under different E. The inset of Fig. 7 shows the luminescence photograph obtained in darkness by a common digital camera.

was also carried out at room temperature. Referring to the optimized PL of BNTO: xSm^{3+} with $x=0.02$, Fig. 7 representatively shows the measured typical polarization—electric field (P—E) hysteresis loops under different external electric fields (E). It is clear that well defined P—E loops can be confirmed in Fig. 7 [27]. It can be seen that the remanent polarization (P_r) is about 32 μC/cm^2 and saturation polarization (P_s) is about 47 μC/cm^2 under $E=110$ kV/cm. It should be noted that obvious reduction of P_r and P_s is observed for BNTO: xSm^{3+} system with the increase of x, for example, $P_r\sim66$ μC/cm^2 and $P_s\sim81$ μC/cm^2 for $x=0.0$ sample. The Bi^{3+} ion with two electrons on the 6s orbital (lone pair) moved away from the centrosymmetric position in its oxygen surrounding, contributing to the overall polarization intensity for BNTO [28]. The substitution of Bi^{3+} ions with Sm^{3+} can lead to the partial break of FE long range order. Thus, the reduction of polarization intensity is confirmed in BNTO: xSm^{3+} system. However, the values of P_r and P_s for BNTO: xSm^{3+} with $x=0.02$ are still much larger than those of the other bismuth layered-structure ferroelectrics [29].

Finally, to evidently indicate the multifunctional features of BNTO: xSm^{3+} with $x=0.02$, the inset of Fig. 7 also gives a luminescence photograph of $x=0.02$ sample obtained in darkness by a common digital camera under the excitation of a blue commercial LED (3 W, 460—470 nm). The strong reddish-orange light emission was clearly observed by naked eyes at room temperature.

4. Conclusion

In conclusion, BNTO: xSm^{3+} ceramics with different Sm^{3+} doped concentrations were synthesized. The structural, photoluminescence, and ferroelectric properties have been carefully investigated. Strong reddish-orange emission which can be excited by both blue light and NUV radiation has been successfully observed. Optimized photoluminescence is realized in BNTO: xSm^{3+} with $x=0.02$ sample which also shows excellent ferroelectric properties. It is believed that BNTO: xSm^{3+} with $x=0.02$ may act as a potentially multifunctional optical-electro-material.

Acknowledgment

This work was supported by the Natural Science Foundation of China (51102277) and Fundamental Research Funds for the Central Universities (ZXH2012P008).

References

[1] A. Bergh, G. Craford, A. Duggal, R. Haitz, The promise and challenge of solid-state lighting, Physics Today 54 (2001) 42.
[2] N. Kimura, K. Sakuma, S. Hirafune, K. Asano, N. Hirosaki, R.-J. Xie, Extrahigh color rendering white light-emitting diode lamps using oxynitride and nitride phosphors excited by blue light-emitting diode, Applied Physics Letters 90 (2007) 051109.
[3] S. Ye, F. Xiao, Y.X. Pan, Y.Y. Ma, Q.Y. Zhang, Phosphors in phosphor-converted white light-emitting diodes: recent advances in materials, techniques and properties, Materials Science and Engineering R 71 (2010) 1–34.
[4] J.K. Sheu, S.J. Chang, C.H. Kuo, Y.K. Su, L.W. Wu, Y.C. Lin, W.C. Lai, J.M. Tsai, G.C. Chi, R.K. Wu, White-light emission from near UV

InGaN—GaN LED chip precoated with blue/green/red phosphors, IEEE Photonics Technology Letters 15 (2003) 18–20.
[5] J.S. Kim, P.E. Jeon, J.C. Choi, H.L. Park, S.I. Mho, G.C. Kim, Warm-white-light emitting diode utilizing a single-phase full-color $Ba_3MgSi_2O_8$:Eu^{2+}, Mn^{2+} phosphor, Applied Physics Letters 84 (2004) 2931.
[6] T. Kyômen, R. Sakamoto, N. Sakamoto, S. Kunugi, M. Itoh, Photoluminescence properties of Pr-doped (Ca,Sr,Ba)TiO_3, Chemistry of Materials 17 (2005) 3200–3204.
[7] S. Okamoto, H. Yamamoto, Characteristic enhancement of emission from $SrTiO_3$:Pr^{3+} by addition of group-IIIb ions, Applied Physics Letters 78 (2001) 655.
[8] X.J. Zhang, J.H. Zhang, Z.G. Nie, M.Y. Wang, X.G. Ren, X.J. Wang, Enhanced red phosphorescence in nanosized $CaTiO_3$:Pr^{3+} phosphors, Applied Physics Letters 90 (2007) 151911.
[9] H. Takashima, K. Ueda, M. Itoh, Red photoluminescence in praseodymium-doped titanate perovskite films epitaxially grown by pulsed laser deposition, Applied Physics Letters 89 (2006) 261915.
[10] C.T. Luo, W.W. Ge, Q.H. Zhang, J.F. Li, H.S. Luo, D. Viehland, Crystallographic direction dependence of direct current field induced strain and phase transitions in $Na_{0.5}Bi_{0.5}TiO_3$—x%$BaTiO_3$ single crystals near the morphotropic phase boundary, Applied Physics Letters 101 (2012) 141912.
[11] J.J. Yao, W.W. Ge, L. Luo, J.F. Li, D. Viehland, H.S. Luo, Hierarchical domains in $Na_{1/2}Bi_{1/2}TiO_3$ single crystals: ferroelectric phase transformations within the geometrical restrictions of a ferroelastic inheritance, Applied Physics Letters 96 (2010) 222905.
[12] W.W. Ge, C.T. Luo, Q.H. Zhang, C.P. Devreugd, Y. Ren, J.F. Li, H. S. Luo, D. Viehland, Ultrahigh electromechanical response in $(1-x)$ $(Na_{0.5}Bi_{0.5})TiO_3$—$x$$BaTiO_3$ single-crystals via polarization extension, Journal of Applied Physics 111 (2012) 093508.
[13] H.Q. Sun, D.F. Peng, X.S. Wang, M.M. Tang, Q.W. Zhang, X. Yao, Strong red emission in Pr doped $(Bi_{0.5}Na_{0.5})TiO_3$ ferroelectric ceramics, Journal of Applied Physics 110 (2011) 016102.
[14] H. Zhou, X. Liu, N. Qin, D.H. Bao, Strong red emission in lead-free ferroelectric Pr^{3+}-doped $Na_{0.5}Bi_{0.5}TiO_3$ thin films without the need of charge compensation, Journal of Applied Physics 110 (2011) 034102.
[15] X.L. Tian, Z. Wu, Y.M. Jia, J.R. Chen, R.K. Zheng, Y.H. Zhang, H. S. Luo, Remanent-polarization-induced enhancement of photoluminescence in Pr^{3+}-doped lead-free ferroelectric $(Bi_{0.5}Na_{0.5})TiO_3$ ceramic, Applied Physics Letters 102 (2013) 042907.
[16] Z.H. Ju, R.P. Wei, J.R. Zheng, X.P. Gao, S.H. Zhang, W.S. Liu, Synthesis and phosphorescence mechanism of a reddish orange emissive long afterglow phosphor Sm^{3+}-doped Ca_2SnO_4, Applied Physics Letters 98 (2011) 121906.
[17] V.R. Bandi, B.K. Grandhe, K. Jang, H.S. Lee, S.S. Yi, J.H. Jeong, Citric based sol—gel synthesis and photoluminescence properties of un-doped and Sm^{3+} doped $Ca_3Y_2Si_3O_{12}$ phosphors, Ceramics International 37 (2011) 2001.
[18] T. Wei, Y.J. Guo, P.W. Wang, D.P. Yu, K.F. Wang, C.L. Lu, J.-M. Liu, Ru doping induced quantum paraelectricity in ferroelectric $Sr_{0.9}Ba_{0.1}$-TiO_3, Applied Physics Letters 92 (2008) 172912.
[19] R.D. Shannon, Revised effective ionic radii and systematic studies of interatomie distances in halides and chaleogenides, Acta Crystallographica A 32 (1976) 751–767.
[20] S. Sailaja, S.J. Dhoble, B.S. Reddy, Synthesis and photoluminescence properties of Sm^{3+} and Dy^{3+} ions activated $Ca_2Gd_2W_3O_{14}$ phosphors, Journal of Molecular Structure 1003 (2011) 115–120.
[21] K.D. Chang, H.J. Lee, H.S. Jang, K.S. Choi, S.Y. Lee, S.D. Choi, Study of photoluminescence in lead tungstates doped with Pr^{3+}, Sm^{3+}, and Er^{3+} ions, Journal of Applied Physics 91 (2002) 2766.
[22] Y. Jin, J.H. Zhang, S.Z. Lu, H.F. Zhao, X. Zhang, X.J. Wang, Fabrication of Eu^{3+} and Sm^{3+} codoped micro/nanosized $MMoO_4$ (M=Ca, Ba, and Sr) via facile hydrothermal method and their photoluminescence properties through energy transfer, Journal of Physical Chemistry C 112 (2008) 5860.
[23] V. Singh, S. Watanabe, T.K.G. Rao, J.F.D. Chubaci, H.Y. Kwak, Luminescence and defect centres in $MgSrAl_{10}O_{17}$:Sm^{3+} phosphor, Journal of Non-Crystalline Solids 356 (2010) 1185–1190.
[24] A.N. Yerpude, S.J. Dhoble, Synthesis and photoluminescence properties of Dy^{3+}, Sm^{3+} activated $Sr_5SiO_4Cl_6$ phosphor, Journal of Luminescence 132 (2012) 2975–2978.
[25] H.K. Yang, J.W. Chung, B.K. Moon, B.C. Choi, J.H. Jeong, S.S. Yi, J. H. Kim, K.H. Kim, Crystalline and photoluminescence characteristics of YVO_4:Sm^{3+} thin films grown by pulsed laser deposition under oxygen pressure, Journal of Luminescence 129 (2009) 492–495.
[26] R. Naik, N. Karanjikar, M. Razvi, Concentration quenching of fluorescence from $^1D_2$ state of Pr^{3+} in YPO_4, Journal of Luminescence 54 (1992) 139–144.
[27] T. Wei, J.-M. Liu, Q.J. Zhou, Q.G. Song, Coupling and competition between ferroelectric and antiferroelectric states in Ca-doped $Sr_{0.9-x}Ba_{0.1}Ca_xTiO_3$: multipolar states, Physical Review B 83 (2011) 052101.
[28] J. Wang, J.B. Neaton, H. Zheng, V. Nagarajan, S.B. Ogale, B. Liu, D. Viehland, V. Vaithyanathan, D.G. Schlom, U.V. Waghmare, N. A. Spaldin, K.M. Rabe, M. Wuttig, R. Ramesh, Epitaxial $BiFeO_3$ multiferroic thin film heterostructures, Science 299 (2003) 1719–1722.
[29] D.F. Peng, H.Q. Sun, X.S. Wang, J.C. Zhang, M.M. Tang, X. Yao, Red emission in Pr doped $CaBi_4Ti_4O_{15}$ ferroelectric ceramics, Materials Science and Engineering: B 176 (2011) 1513–1516.